International Journal of Remote Sensing
Vol. 00, No. 00, DD Month 200x, 1–10

An Improved Intensity-Hue-Saturation Method for IKONOS Image Fusion

M.-J Choi*[†‡] , H.-C. Kim[§], N. I. Cho[§] and H. O. Kim[‡]
[†]Satellite Technology Research Center, Korea Advanced Institute of Science and Technology, Daejeon, 305-701, Republic of KOREA.
[‡] Division of Applied Mathematics, Korea Advanced Institute of Science and Technology, Daejeon, 305-701, Republic of KOREA.
[§] School of Electrical Engineering and Computer Science, Seoul National University, Seoul, 151-744, Republic of KOREA.

(*Received 00 Month 200x; In final form 00 Month 200x*)

A useful technique in various applications of remote sensing involves the fusion of panchromatic (Pan) and multispectral (MS) satellite images. Recently, Tu *et al.* introduced a fast intensity-hue-saturation (FIHS) method of image fusion with spectral adjustment for IKONOS imagery. Aside from its fast computing capability for fusing images, this method can help overcome the color distortion problem inherent in IHS-like fusion. Because the spectral response of an IKONOS Pan image does not cover the spectral response of the blue and green band, Tu *et al.* used the FIHS method in a special way: that it, they applied a modified intensity image with weighting parameters of 0.75 for the green band and 0.25 for the blue band. However, because the response of the IKONOS Pan image extends far beyond the near-infrared (NIR) band, additional spectral adjustment of the NIR band is desirable. We therefore propose an FIHS method that incorporates spectral adjustment of all IKONOS MS bands. The proposed approach performs better than the approach of Tu *et al.* and provides a satisfactory result, both visually and quantitatively.

1 Introduction

The fusion of a panchromatic (Pan) image with a high spatial and low spectral resolution and multispectral (MS) images with a low spatial and high spectral resolution has become a powerful tool in many remote sensing applications that require both high spatial and high spectral resolution, such as feature detection, change monitoring, urban analysis, land cover classification, and recently GIS-based applications.

In the remote sensing community, probably the most popular image fusion method is the intensity-hue-saturation (IHS) fusion technique which has been used as a standard procedure in many commercial packages (Carper *et al.*, 1990; Chavez *et al.*, 1991). Recently, Tu *et al.* (2001) introduced a fast IHS fusion (FIHS) method. In general, the IHS fusion method converts a color image from the red, green, and blue (RGB) space into the IHS color space. The intensity (I) band in the IHS space is replaced by a high-resolution Pan image and then transformed back into the original RGB space together with the previous hue (H) band and the saturation (S) band, resulting in an IHS fused image. However, the IHS method can be easily implemented by the procedure which the fused images can be obtained by adding the difference image between Pan and I images to the MS images, respectively. Aside from its fast computing capability for fusing images, this method can extend traditional three-order transformation to an arbitrary order. It can also quickly merge massive volumes of data by requiring only resampled MS data. That is, it is well suited in terms of processing speed for merging high-resolution satellite images (such as IKONOS, QuickBird, KOMPSAT2). However, the FIHS fusion also distorts color in the same way as fusion processes such as the IHS fusion technique. In particular, the large difference between the values of Pan and I appears to cause the large spectral distortion of fused images.

In contrast, the wavelet-based fusion method, which is widely used as an image fusion technique, is based on multiresolution analysis (Yocky, 1996; Zhou *et al.*, 1998; Chibani *et al.*, 2002). The wavelet

Corresponding author. Email: prime@satrec.kaist.ac.kr

approach preserves the spectral characteristics of the MS image better than the IHS method. In general, however, images fused by wavelets have much less spatial information than those fused by the IHS method. Moreover, the wavelet-based fusion method is not efficient enough to quickly merge massive volumes of data from high-resolution satellite images because of its high computational complexity.

The fast computing needs of IKONOS image fusion have recently led to the introduction of methods based on FIHS fusion. Tu *et al.* (2004) presented a simple spectral-adjusted scheme based on an extended FIHS method for IKONOS imagery. They minimized the spectral distortion inherent in IHS-like methods by using a modified I image with spectral adjustment. To modify the I image, they considered two spectral mismatches: namely, that the G band is not fully covered by the spectral response of the IKONOS Pan band, and that the B band mostly falls outside the 3 dB level of the IKONOS Pan band. According to their experimental results, the best weighting parameters were 0.75 for the G band and 0.25 for the B band. Their approach can provide a better performance than the original IHS method, both in processing speed and image quality. Nevertheless, the spectral distortion problem is not completely overcome. That is, the color distortion is slightly apparent on buildings, roads, and bare soil areas in fused images.

On the other hand, because the response of the IKONOS Pan extends far beyond the near-infrared (NIR) band, we need to consider additional spectral adjustment for the NIR band. We therefore propose an extended FIHS method in which spectral adjustment is considered for all IKONOS MS bands. The proposed approach performs better than the approach of Tu *et al.* In addition, it produces results that are more satisfactory than the results of either the wavelet-based approach to spectral resolution of fused images or the FIHS approach to spatial resolution of fused images.

2 IHS-Based Fusion Technique

2.1 *IHS fusion method*

The IHS fusion for each pixel can be formulated by the following procedure:

Step 1)

$$\begin{bmatrix} \mathrm{I} \\ v_1 \\ v_2 \end{bmatrix} = \begin{bmatrix} \frac{1}{3} & \frac{1}{3} & \frac{1}{3} \\ \frac{-\sqrt{2}}{6} & \frac{-\sqrt{2}}{6} & \frac{2\sqrt{2}}{6} \\ \frac{1}{\sqrt{2}} & \frac{-1}{\sqrt{2}} & 0 \end{bmatrix} \begin{bmatrix} \mathrm{R} \\ \mathrm{G} \\ \mathrm{B} \end{bmatrix}. \tag{1}$$

Step 2) The intensity component I is replaced by the Pan image.
Step 3)

$$\begin{bmatrix} \mathrm{F(R)} \\ \mathrm{F(G)} \\ \mathrm{F(B)} \end{bmatrix} = \begin{bmatrix} 1 & \frac{-1}{\sqrt{2}} & \frac{1}{\sqrt{2}} \\ 1 & \frac{-1}{\sqrt{2}} & \frac{-1}{\sqrt{2}} \\ 1 & \sqrt{2} & 0 \end{bmatrix} \begin{bmatrix} \mathrm{Pan} \\ v_1 \\ v_2 \end{bmatrix} = \begin{bmatrix} 1 & \frac{-1}{\sqrt{2}} & \frac{1}{\sqrt{2}} \\ 1 & \frac{-1}{\sqrt{2}} & \frac{-1}{\sqrt{2}} \\ 1 & \sqrt{2} & 0 \end{bmatrix} \begin{bmatrix} \mathrm{I} + (\mathrm{Pan} - \mathrm{I}) \\ v_1 \\ v_2 \end{bmatrix} = \begin{bmatrix} \mathrm{R} + (\mathrm{Pan} - \mathrm{I}) \\ \mathrm{G} + (\mathrm{Pan} - \mathrm{I}) \\ \mathrm{B} + (\mathrm{Pan} - \mathrm{I}) \end{bmatrix}, \tag{2}$$

where F(X) is the fused image of the X band, for $\mathrm{X} = \mathrm{R}, \mathrm{G}, \mathrm{B}$, respectively.

Equation (2) states that the fused image $[\mathrm{F(R)}, \mathrm{F(G)}, \mathrm{F(B)}]^{\mathrm{T}}$ can be easily obtained from the original image $[\mathrm{R}, \mathrm{G}, \mathrm{B}]^{\mathrm{T}}$ simply by using addition operations. That is, the IHS method can be implemented efficiently by this procedure. This method is called the fast IHS fusion method.

The problem with the IHS method is that spectral distortion may occur during the merging process. In Eq.(2), the large difference between the values of Pan and I appears to cause the large spectral distortion of fused images. Indeed, this difference $(\mathrm{Pan} - \mathrm{I})$ causes the altered saturation component in the RGB-IHS conversion model.

In an RGB-IHS conversion model, the saturation component (S) can be represented as follows:

$$\mathrm{S} = 1 - \frac{3\min\{\mathrm{R}, \mathrm{G}, \mathrm{B}\}}{\mathrm{R} + \mathrm{G} + \mathrm{B}} = \frac{\mathrm{I} - \mathrm{X}_0}{\mathrm{I}}, \tag{3}$$

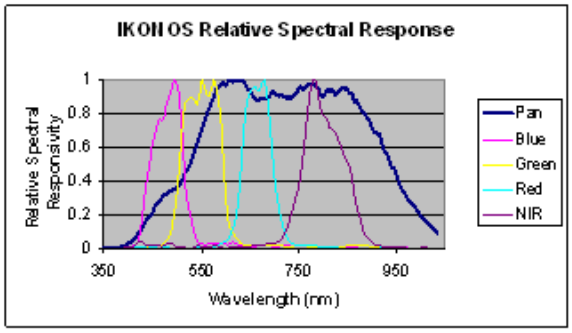

Figure 1. Relative spectral responses of IKONOS image

where X_0 is the smallest value among R, G, and B for each pixel.

The new saturation value for the image fused by the IHS method then becomes

$$S_{IHS} = 1 - \frac{3\min\{R+\delta, G+\delta, B+\delta\}}{R+G+B+3\delta} = 1 - \frac{X_0+\delta}{Pan} = \frac{I-X_0}{Pan}, \tag{4}$$

where $\delta = Pan - I$.

The relation between Eq.(3) and Eq.(4) is

$$\frac{S_{IHS}}{S} = \frac{\frac{I-X_0}{Pan}}{\frac{I-X_0}{I}} = \frac{I}{Pan} = \frac{I}{I+\delta}. \tag{5}$$

This δ parameter is therefore a crucial factor in the spectral distortion problem when the difference between the values of Pan and I is large (see Tu *et al.*, 2001, 2004, and references therein).

2.2 *IKONOS image fusion*

When IHS-like fusion methods are used with IKONOS imagery, there is a significant color distortion, due primarily to the range of wavelengths in an IKONOS Pan image. Unlike the Pan images of SPOT and IRS sensors, IKONOS Pan images (as shown Fig. 1) have an extensive range of wavelengths-from visible to near-infrared. This difference obviously induces the color distortion problem in IHS fusion as a result of the mismatches; that is, the Pan and I are spectrally dissimilar (Zhang, 2004). In particular, the grey values of Pan in the green vegetated regions are far larger than the grey values of I because the areas covered by vegetation are characterized by a relatively high reflectance of NIR and Pan bands as well as a low reflectance in the RGB bands. To minimize the radiance differences between Pan and I, Tu *et al.* (2004) included the NIR band in the definition of the I component. Indeed, the fusion algorithm proposed by Tu *et al.* reduces the color distortions in fused images, especially on vegetated areas. This way, and motivated by (2), the FIHS method can be extended from three to four bands by

$$\begin{bmatrix} F(R) \\ F(G) \\ F(B) \\ F(NIR) \end{bmatrix} = \begin{bmatrix} R+\delta' \\ G+\delta' \\ B+\delta' \\ NIR+\delta' \end{bmatrix}, \tag{6}$$

where $\delta' = Pan - I'$ and $I' = (R+G+B+NIR)/4$.

We call this method the eFIHS method.

2.3 *New FIHS-based methods for IKONOS image fusion*

In addition, Tu *et al.* (2004) introduced eFIHS with spectral adjustment (eFIHS SA) applied to the I image, considering that

$$\delta'' = \mathrm{Pan} - \mathrm{I}'' = \mathrm{Pan} - \frac{\mathrm{R} + \mathrm{a} * \mathrm{G} + \mathrm{b} * \mathrm{B} + \mathrm{NIR}}{3}, \tag{7}$$

where a and b are weighting parameters defined to take into account that the spectral response of the Pan image does not cover that of the blue and green band. The value of these parameters was estimated experimentally after the fusion of 92 IKONOS images, covering different areas. According to the experimental results obtained by Tu *et al.*, the best weighting parameters of a and b for G and B bands are 0.75 and 0.25, respectively.

Recently, González-Audícana *et al.* (2006) introduced a low computation-cost method to fuse IKONOS images using the spectral response function (SRF) of its sensors based on the eFIHS method. The method proposed by González-Audícana *et al.* (eFIHS SRF) can be represented by

$$\begin{bmatrix} \mathrm{F(R)} \\ \mathrm{F(G)} \\ \mathrm{F(B)} \\ \mathrm{F(NIR)} \end{bmatrix} = \begin{bmatrix} \mathrm{R} + ((\mathrm{I_{new}} - \mathrm{I}') \cdot \mathrm{R}/\mathrm{I}') \\ \mathrm{G} + ((\mathrm{I_{new}} - \mathrm{I}') \cdot \mathrm{G}/\mathrm{I}') \\ \mathrm{B} + ((\mathrm{I_{new}} - \mathrm{I}') \cdot \mathrm{B}/\mathrm{I}') \\ \mathrm{NIR} + ((\mathrm{I_{new}} - \mathrm{I}') \cdot \mathrm{NIR}/\mathrm{I}') \end{bmatrix} = \begin{bmatrix} (\mathrm{I_{new}}/\mathrm{I}') \cdot \mathrm{R} \\ (\mathrm{I_{new}}/\mathrm{I}') \cdot \mathrm{G} \\ (\mathrm{I_{new}}/\mathrm{I}') \cdot \mathrm{B} \\ (\mathrm{I_{new}}/\mathrm{I}') \cdot \mathrm{NIR} \end{bmatrix}, \tag{8}$$

where $\mathrm{I_{new}} = (1/4) \cdot \gamma \cdot \mathrm{Pan}$.

The value γ just depends on the SRF of the Pan and MS sensors, being independent of the images to be fused. This value is near 0.80 for the IKONOS satellite sensors.

At the same time, Choi (2006) proposed a new FIHS fusion approach to Image fusion with a tradeoff parameter. The approach based on the eFIHS method (eFIHS TP) is expressed as follows:

$$\begin{bmatrix} \mathrm{F(R)} \\ \mathrm{F(G)} \\ \mathrm{F(B)} \\ \mathrm{F(NIR)} \end{bmatrix} = \begin{bmatrix} \mathrm{R} + t \cdot \delta' \\ \mathrm{G} + t \cdot \delta' \\ \mathrm{B} + t \cdot \delta' \\ \mathrm{NIR} + t \cdot \delta' \end{bmatrix}, \tag{9}$$

where t are a tradeoff parameter in the interval [0,1]. In the approach, the tradeoff parameter is used to control the tradeoff between the spatial and spectral resolution of the image to be fused. Therefore, with an appropriate tradeoff parameter, the approach provided a satisfactory result as well as wavelet-based approaches, both visually and quantitatively. However, Choi did not give an explicit algorithm for choosing an appropriate tradeoff parameter that corresponds to a given application. This drawback presupposes considerable trial and error for choosing an appropriate tradeoff parameter. In this work, we use 0.8 as a well-suited tradeoff parameter for IKONOS image fusion.

2.4 *The proposed method*

The proposed method is expressed as follows:

$$\begin{bmatrix} \mathrm{F(R)} \\ \mathrm{F(G)} \\ \mathrm{F(B)} \\ \mathrm{F(NIR)} \end{bmatrix} = \begin{bmatrix} \mathrm{R} + \delta''' \\ \mathrm{G} + \delta''' \\ \mathrm{B} + \delta''' \\ \mathrm{NIR} + \delta''' \end{bmatrix}, \tag{10}$$

where $\delta''' = \mathrm{Pan} - \mathrm{I}''' = \mathrm{Pan} - \frac{\mathrm{a}*\mathrm{R}+0.75\cdot\mathrm{G}+0.25\cdot\mathrm{B}+\mathrm{b}*\mathrm{NIR}}{3}$.

We used the same weighting parameters as those of the eFIHS SA method for the G and B bands. The reason for using these weighting parameters is that they don't affect the choice of parameters for the

Table 1. Average ERGAS values of 29 IKONOS sets between resampled and fused images, varying with spectral weights

a	0.2	0.25	0.3	0.35	0.4	0.45	0.5
b	1.8	1.75	1.7	1.65	1.6	1.55	1.5
	3.4332	3.4265	3.4234	3.4240	3.4284	3.4367	3.4493

proposed method because the R and NIR bands don't overlap with the G and B bands. Hence, we only had to find the appropriate weighting parameters for the R and NIR bands. Similarly to the eFIHS SA method, we experimentally estimated the value of these parameters after the fusion of 29 IKONOS sets, which covered different areas. For simplification, we assumed that $a + b = 2$ and $a < b$. Furthermore, to determine the values of a and b, we used as an index the erreur relative globale adimensionnelle de synthese (ERGAS), which means the relative global dimensional synthesis error, between the fused image and the original MS image (including the R, G, B, and NIR bands). Table 1 lists the average values of ERGAS for the 29 IKONOS sets. In the table, the value of a increases from 0.2 to 0.5 in steps of 0.05. According to experimental results, the best weighting parameters for the R and NIR bands are 0.3 for a and 1.7 for b.

2.5 *eFIHS-based wavelets method*

González-Audícana *et al.* (2004), recently, introduced a hybrid algorithm, which used the additive wavelet on the intensity method. They used multiresolution wavelet decomposition to execute the detailed extraction phase, and they followed the IHS procedure to inject the spatial detail of the Pan image into the MS image. In other words, instead of using the Pan image in Eq. (2), they used the fusion results of the Pan image and the intensity image fused by the additive wavelet method (see Núñez *et al.* (1999); González-Audícana *et al.* (2005) for the additive wavelet method). If this hybrid algorithm is based on eFIHS method, it can be much simpler and faster than original algorithm. The hybrid algorithm based on eFIHS method is expressed as follows (see González-Audícana *et al.* (2006)):

$$\begin{bmatrix} \mathrm{F(R)} \\ \mathrm{F(G)} \\ \mathrm{F(B)} \\ \mathrm{F(NIR)} \end{bmatrix} = \begin{bmatrix} \mathrm{R} + (\mathrm{I}'_{\mathrm{new}} - \mathrm{I}') \\ \mathrm{G} + (\mathrm{I}'_{\mathrm{new}} - \mathrm{I}') \\ \mathrm{B} + (\mathrm{I}'_{\mathrm{new}} - \mathrm{I}') \\ \mathrm{NIR} + (\mathrm{I}'_{\mathrm{new}} - \mathrm{I}') \end{bmatrix} = \begin{bmatrix} \mathrm{R} + \sum_{k=1}^{n} \mathrm{W}_{\mathrm{Pan}_k} \\ \mathrm{G} + \sum_{k=1}^{n} \mathrm{W}_{\mathrm{Pan}_k} \\ \mathrm{B} + \sum_{k=1}^{n} \mathrm{W}_{\mathrm{Pan}_k} \\ \mathrm{NIR} + \sum_{k=1}^{n} \mathrm{W}_{\mathrm{Pan}_k} \end{bmatrix}, \tag{11}$$

where $\mathrm{I}'_{\mathrm{new}} = \mathrm{I}' + \sum_{k=1}^{n} \mathrm{W}_{\mathrm{Pan}_k}$ and $\sum_{k=1}^{n} \mathrm{W}_{\mathrm{Pan}_k}$ is the sum of the high-frequency versions of the wavelet-transformed Pan image. In this work, we use the *à trous* algorithm (see Dutilleux, 1989, and references therein) with a B-cubic spline profile for the wavelet transform.

3 Experimental Study and Analysis

To merge an IKONOS Pan image and MS images, we used an image acquired on 9 March 2002 of the Korean city of Daejeon. Next, we used two sets of IKONOS images, with one set featuring an agricultural area and the other featuring a city area, and we used the two sets to evaluate the performance of the proposed image fusion method and to compare it with other fusion methods.

3.1 *The factors of quantitative analysis*

Our quantitative analysis is based on the experimental results of the factors used in (Zhou *et al.*, 1998; Ranchin *et al.*, 2003; Choi *et al.*, 2005): namely, the standard deviation (SD); the correlation coefficients (CCs); the relative average spectral error (RASE); ERGAS; and the spatial quality measurement proposed by Zhou *et al.* These estimators are commonly used to assess the spectral and spatial quality of fused images.

- The SD of the difference image in relation to the mean of the original image indicates the level of the

error at any pixel. The lower the value of this parameter, the better the spectral quality of the fused image.

- The CC between the original image and the fused image is defined as

$$\mathrm{CC}(A,B) = \frac{\sum_{m,n}(A_{mn}-\overline{A})(B_{mn}-\overline{B})}{\sqrt{(\sum_{m,n}(A_{mn}-\overline{A})^2)(\sum_{m,n}(B_{mn}-\overline{B})^2)}}, \tag{12}$$

where $\overline{A}$ and $\overline{B}$ stand for the mean values of the corresponding data set, and CC is calculated globally for the entire image. The result of this equation shows similarity in the small structures between the original image and the fused image.

- To estimate the global spectral quality of the fused images, we expressed the index of the RASE as a percentage. By characterizing the average performance of the method of image fusion in the spectral bands considered, the percentage is expressed as follows:

$$\mathrm{RASE} = \frac{100}{M}\sqrt{\frac{1}{N}\sum_{i=1}^{N} RMSE^2(B_i)}, \tag{13}$$

where M is the mean radiance of the N spectral bands (B_i) of the original MS bands, and $RMSE$ is the root mean square error. The $RMSE$ value is as computed as follows:

$$RMSE^2(B_i) = bias^2(B_i) + SD^2(B_i). \tag{14}$$

The ERGAS index for the fusion is expressed as follows:

$$\mathrm{ERGAS} = 100\frac{h}{l}\sqrt{\frac{1}{N}\sum_{i=1}^{N}\frac{RMSE^2(B_i)}{M_i^2}}, \tag{15}$$

where h is the resolution of the high spatial resolution image, l is the resolution of the low spatial resolution image, and M_i is the mean radiance of each spectral band involved in the fusion. The lower the value of the RASE index and the ERGAS index, the higher the spectral quality of the fused images.

- To evaluate the detailed spatial information, we use a procedure proposed by Zhou *et al.* In this procedure, we filtered the Pan and fused images with a Laplacian filter as follows:

$$\begin{pmatrix} -1 & -1 & -1 \\ -1 & 8 & -1 \\ -1 & -1 & -1 \end{pmatrix}. \tag{16}$$

The high correlation coefficients between the fused filtered image and the Pan filtered image (sCCs) indicate that most of the spatial information of the Pan image was incorporated during the merging process. The sCC has the same definition as the CC.

3.2 *Quantitative analysis*

To assess the spectral and spatial quality of the fused images, we derived spatially degraded Pan and MS images from the original images. For the experiment on the fusion of IKONOS images, the derived images have a resolution of 4 m and 16 m, respectively. These images were synthesized at a 4 m resolution and then compared to the original IKONOS MS images.

With respect to the five factors referred to in section 3.1, Tables 2 and 3 compare the experimental image fusion results of the introduced methods.

Table 2. Comparative 1^{st}IKONOS fusion results

		Initial	eFIHS	eFIHS SA	eFIHS SRF	eFIHS TP	eFSWI W	Pro-posed
SD(%)	R	14.721	11.869	10.446	11.607	10.656	9.2027	9.7044
(ideal:0)	G	13.654	11.629	10.573	12.417	9.9050	8.5902	9.5558
	B	14.575	15.520	14.750	13.604	12.570	10.560	12.583
		18.246	12.989	11.853	11.807	12.514	10.285	9.5354
	NIR							
$\overline{\text{SD}}$		**15.299**	**13.001**	**11.905**	**12.358**	**11.411**	**9.6594**	**10.344**
CC	R	0.9349	0.9576	0.9672	0.9595	0.9659	0.9745	0.9717
(ideal:1)	G	0.9436	0.9591	0.9662	0.9533	0.9703	0.9776	0.9723
	B	0.9442	0.9367	0.9428	0.9513	0.9585	0.9707	0.9584
		0.8471	0.9225	0.9354	0.9359	0.9281	0.9514	0.9582
	NIR							
$\overline{\text{CC}}$		**0.9174**	**0.9439**	**0.9529**	**0.9500**	**0.9557**	**0.9685**	**0.9651**
sCC	R	0.3038	0.9982	0.9984	0.9907	0.9934	0.9931	0.9959
	G	0.2968	0.9989	0.9984	0.9933	0.9953	0.9931	0.9963
	B	0.2847	0.9972	0.9960	0.9830	0.9962	0.9938	0.9952
		0.3245	0.9949	0.9962	0.9647	0.9891	0.9950	0.9982
	NIR							
$\overline{\text{sCC}}$		**0.3024**	**0.9973**	**0.9972**	**0.9829**	**0.9935**	**0.9937**	**0.9964**
		15.863	12.929	11.818	12.347	11.536	9.7304	10.202
RASE(%)								
ERGAS		**3.8497**	**3.2733**	**3.0078**	**3.0959**	**2.8676**	**2.4232**	**2.6063**

Table 3. Comparative 2^{nd}IKONOS fusion results

		Initial	eFIHS	eFIHS SA	eFIHS SRF	eFIHS TP	eFSWI W	Pro-posed
SD(%)	R	28.101	15.060	13.935	14.758	15.709	15.738	14.580
(ideal:0)	G	22.473	12.845	12.310	13.483	12.274	12.329	12.289
	B	19.119	15.220	15.075	15.914	13.048	12.133	14.297
		38.779	21.157	19.735	22.916	22.375	20.491	17.639
	NIR							
$\overline{\text{SD}}$		**27.118**	**16.070**	**15.263**	**16.767**	**15.851**	**15.172**	**14.701**
CC	R	0.7616	0.9315	0.9413	0.9342	0.9255	0.9252	0.9358
(ideal:1)	G	0.7800	0.9281	0.9340	0.9208	0.9343	0.9338	0.9342
	B	0.8139	0.8820	0.8843	0.8710	0.9133	0.9250	0.8959
		0.7210	0.9169	0.9277	0.9025	0.9071	0.9221	0.9422
	NIR							
$\overline{\text{CC}}$		**0.7691**	**0.9146**	**0.9218**	**0.9071**	**0.9200**	**0.9265**	**0.9270**
sCC	R	0.2763	0.9966	0.9975	0.9891	0.9922	0.9921	0.9952
	G	0.2643	0.9978	0.9974	0.9946	0.9944	0.9924	0.9961
	B	0.2353	0.9967	0.9952	0.9854	0.9946	0.9929	0.9949
		0.2953	0.9970	0.9974	0.9575	0.9944	0.9964	0.9989
	NIR							
$\overline{\text{sCC}}$		**0.2678**	**0.9970**	**0.9968**	**0.9816**	**0.9939**	**0.9934**	**0.9962**
		27.221	15.930	15.136	16.685	15.780	15.091	14.590
RASE(%)								
ERGAS		**7.0313**	**4.0910**	**3.8780**	**4.2903**	**4.0858**	**3.8867**	**3.7063**

3.2.1 ***Comparative analysis of the eFIHS method and the proposed method of IKONOS image fusion.*** Compared with the proposed method, as shown in Tables 2 and 3, the eFIHS method has higher values for the SD, RASE, and ERGAS but a lower value for the CC. This result, which is likely due to the non-ideal spectral responses of IKONOS imagery, means that the images fused by the eFIHS method have lower spectral quality than images fused by the proposed method. Ideally, the RGB bands should fall just within the spectral range of the Pan band. In Fig. 1, the G and B bands appear to overlap substantially, and the B band mostly falls outside of the Pan band. Furthermore, the response of the Pan band extends far beyond the NIR band, thereby inducing the color distortion in IHS-like fusion. To cope with this problem, we considered additional spectral adjustment for all IKONOS MS bands. The proposed method is very suitable for IKONOS image fusion, and the experimental results of Table 2 and 3 support this fact. Thus, in IHS-like image fusion, the precise choice of intensity component clearly affects the performance of image fusion.

(a) (b) (c) (d)

Figure 2. Results for 1^{st} (a) The 1^{st} IKONOS Pan image (degraded to 4m) (b) The 1^{st} initial color image(degraded to 16m and resampled to 4m); a) The 2^{nd} IKONOS Pan image (degraded to 4m) (b) The 2^{nd} initial color image(degraded to 16m and resampled to 4m).

3.2.2 ***Comparative analysis of the eFSWI method and the proposed method of IKONOS image fusion.*** Compared with the proposed method, as shown in Table 2, the eFSWI method has lower values for the SD, RASE and ERGAS but a slightly higher value for the CC. In contrast, as shown in Table 3, the eFSWI method has higher values than the proposed method for the SD, RASE, and ERGAS but a slightly lower value for the CC. This difference is due solely to the difference between the agricultural area and the city area. According to the literature, wavelet-based methods generally perform better than IHS-like methods, particularly in terms of spectral quality. It is surprising, therefore, to find that the spectral quality of images fused with the proposed method is as good as the spectral quality of images fused with the wavelet-based method.

3.2.3 ***Comparative analysis of the proposed method and other methods of IKONOS image fusion.*** Compared to the eFIHS SA method, the eFIHS SRF method, and the eFIHS TP method, as shown in Tables 2 and 3, the proposed method has lower values for the SD, RASE and ERGAS but greater values of the CC. Hence, the spectral quality of images fused by the proposed method is much better than the spectral quality of images fused by the eFIHS SA method, the eFIHS SRF method, or the eFIHS TP method. Moreover, given that the sCC values of the proposed method are similar to (or slightly lower than) the sCC values of the eFIHS SA method, we can deduce that the proposed method produces a satisfactory spatial resolution.

3.2.4 ***The potential of the proposed method for IKONOS image fusion.*** Although IHS-like methods of image fusion generally offer a fast computing capability and a satisfactory spatial resolution, they tend to produce some distortion in the spectral characteristics of the original MS images. Recently, developments in wavelet analysis have provided a potential solution to this problem. The wavelet approach preserves the spectral characteristics of MS images better than the IHS method, though images fused by wavelet-based methods contain much less spatial information than images fused by IHS methods. Moreover, wavelet-based methods are not efficient enough to handle the high computational complexity of quickly merging massive volumes of data from new satellite images.

Since the proposed method is an IHS-like method, it can provide a fast computing capability and a satisfactory spatial resolution for fusing images. In addition, the experimental results demonstrate that the spectral quality of images fused by the proposed method is as good as the spectral quality of images fused by the wavelet-based method. The proposed method can therefore be used as alternative to the two popular approaches to image fusion.

3.3 *Visual analysis*

Figure 2 shows the degraded Pan images and the corresponding initial RGB images. Most of the test site in Fig. 2(a) includes the agricultural area, and Figs. 3(b) to 3(g) show the fusion results. In spite of the difficulty of determining which fusion method produces images with the best spatial and spectral quality, most fusion methods produce images with a better spatial and spectral quality than the original color image. Furthermore, the color distortion of images fused by the eFIHS method, the eFIHS SA method, the eFIHS SRF method, the eFIHS TP method, and the proposed method is mitigated by the inclusion of the NIR band and consideration of the spectral adjustment. Moreover, all these methods produce a more satisfactory visual quality than the eFIHS W method.

For further verification, we included complicated land covers, such as buildings, roads, and railway lines, in the test area shown in Fig. 2(c). Figures 4(b) to 4(g) show the fusion results. Unlike the results of Fig. 3, most fusion methods produce a satisfactory visual quality for IKONOS image fusion, even though images fused by the eFIHS TP method and the eFIHS W method have a slightly more unsatisfactory spatial quality than images fused by other methods.

4 Conclusion

The fast computing needs of IKONOS image fusion have recently led to the introduction of methods based on FIHS fusion. Tu et al., for example, has presented a simple spectral-adjusted scheme based on an extended FIHS method for IKONOS imagery. Even though the eFIHS SA method gives a satisfactory result for IKONOS image fusion, we can achieve better results through our proposed FIHS method in which additional spectral adjustment is considered for all IKONOS MS bands. To analyze the spatial and spectral quality of the resulting images, we used five factors, namely the SD, CC, RASE, ERGAS, and sCC, and compared the results with the quality of images fused by other methods of image fusion. The experimental results show that images fused by the proposed method have a better spectral quality than images by the eFIHS SA method. Furthermore, the spectral quality of images fused by the proposed method is as good as the spectral quality of images fused by the wavelet-based method. Thus, with its fast computing capability, the proposed method is very suitable for IKONOS image fusion.

Acknowledgment

The authors would like to thank Dr. Kwanghoon Chi of the Korea Institute of Geoscience and Mineral Resources for providing the IKONOS images for this research.

References

Carper, W.J., Lillesand, T.M. and Kiefer, R.W., 1990, The use of intensity-hue-saturation transformations for merging SPOT panchromatic and multispectral image data. *Photogrammetric Engineering and Remote Sensing,* **56**, 459–467.

Chavez, P.S., Sides, S.C. and Anderson, J.A., 1991, Comparison of three difference methods to merge multiresolution and multisepctral data: Landsat TM and SPOT panchromatic. *Photogrammetric Engineering and Remote Sensing,* **57**, 295–303.

Chibani, Y. and Houacine, A., 2002, The joint use of IHS transform and redundant wavelet decomposition for fusing multispectral and panchromatic images. *International Journal of Remote Sensing,* **23**, 3821–3833.

Choi, M., Kim, R.Y., Nam, M.Y. and Kim, H.O., 2005, Fusion of Multispectral and Panchromatic Satellite Images Using the Curvelet Transform. *IEEE Geoscience and Remote sensing letters,* **2**, 136–140.

Choi, M., 2006, A New Intensity-Hue-Saturation Fusion Approach to Image Fusion with a Tradeoff Parameter. *IEEE Transactions on Geoscience and Remote sensing,* **44**, 1672–1682.

Dutilleux, P., 1989, An implementation of the "algorithme à trous" to compute the wavelet transform. In: *Wavelets: Time-Frequency Methods and Phase Space*, J.M. Combes and A. Grossman, and Ph. Tchamitchian, (Eds) (Berlin, Germany: Springer-Verlag), pp. 298–304.

González-Audícana, M., Saleta, J.L., Catal, R.G. and García, R., 2004, Fusion of Multispectral and Panchromatic Images Using Improved IHS and PCA Mergers Based on Wavelet Decomposition. *IEEE Transactions on Geoscience and Remote sensing,* **42**, 1291–1299.

González-Audícana, M., Otazu, X., Fors, O. and Seco, A., 2005, Comparison between Mallat's and the 'à trous' discrete wavelet transform based algorithms for the fusion of multispectral and panchoromatic images. *International Journal of Remote Sensing,* **26**, 595–614.

González-Audícana, M., Otazu, X., Fors, O. and Alvarez-Mozos, J., 2006, A Low Computational-Cost Method to Fuse IKONOS Images Using the Spectral Response Function of Its Sensors. *IEEE Transactions on Geoscience and Remote sensing,* **44**, 1683–1691.

Núñez, J., Otazu, X., Fors, O., Prades, A., Palà, V. and Arbiol, R., 1999, Multiresolution-based image fusion with addtive wavelet decomposion. *IEEE Transactions on Geoscience and Remote sensing,* **37**, 1204–1211.

Ranchin, T., Aiazzi, B., Alparone, L., Baronti, S. and Wald, L., 2003, Image fusion - the ARSIS concept and some successful implementation schemes. *ISPRS Journal of Photogrammetry and Remote Sensing,* **58**, 4–18.

Tu, T.M., Su, S.C., Shyn, H.C. and Huang, P.S., 2001, A new look at IHS-like image fusion methods. *Information Fusion,* **2**, 177–186.

Tu, T.M., Huang, P.S., Hung, C.L. and Chang, C.P., 2004, A Fast Intensity-Hue-Saturation Fusion Technique With Spectral Adjustment for IKONOS Imagery. *IEEE Geoscience and Remote sensing letters,* **1**, 309–312.

Yocky, D.A., 1996, Multiresolution wavelet decomposition image merger of Landsat Thematic Mapper and SPOT panchromatic data. *Photogrammetric Engineering and Remote Sensing,* **62**, 1067–1074.

Zhou, J., Civco, D.L. and Silander, J.A., 1998, A wavelet transform method to merge Landsat TM and SPOT panchromatic data. *International Journal of Remote Sensing,* **19**, 743–757.

Zhang, Y., 2004, Understanding Image Fusion. *Photogrammetric Engineering and Remote Sensing,* **70**, 653–760.

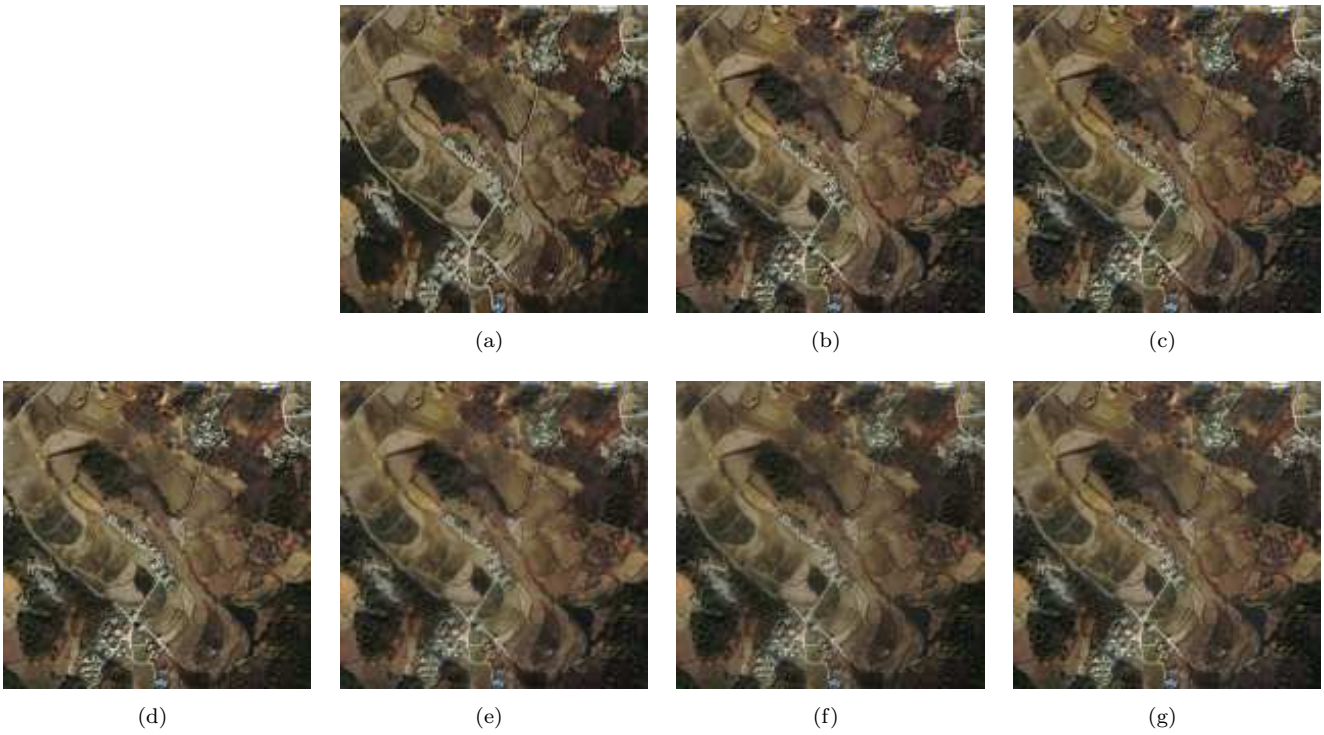

(a) (b) (c)

(d) (e) (f) (g)

Figure 3. Results for 1^{st} IKONOS imagery: (a) original IKONOS color image(4m); (b) fused by the eFIHS; (c) fused by the eFIHS SA; (d) fused by the eFIHS SRF; (e) fused by the eFIHS TP; (f) fused by the eFIHS W; (g) fused by the proposed method.

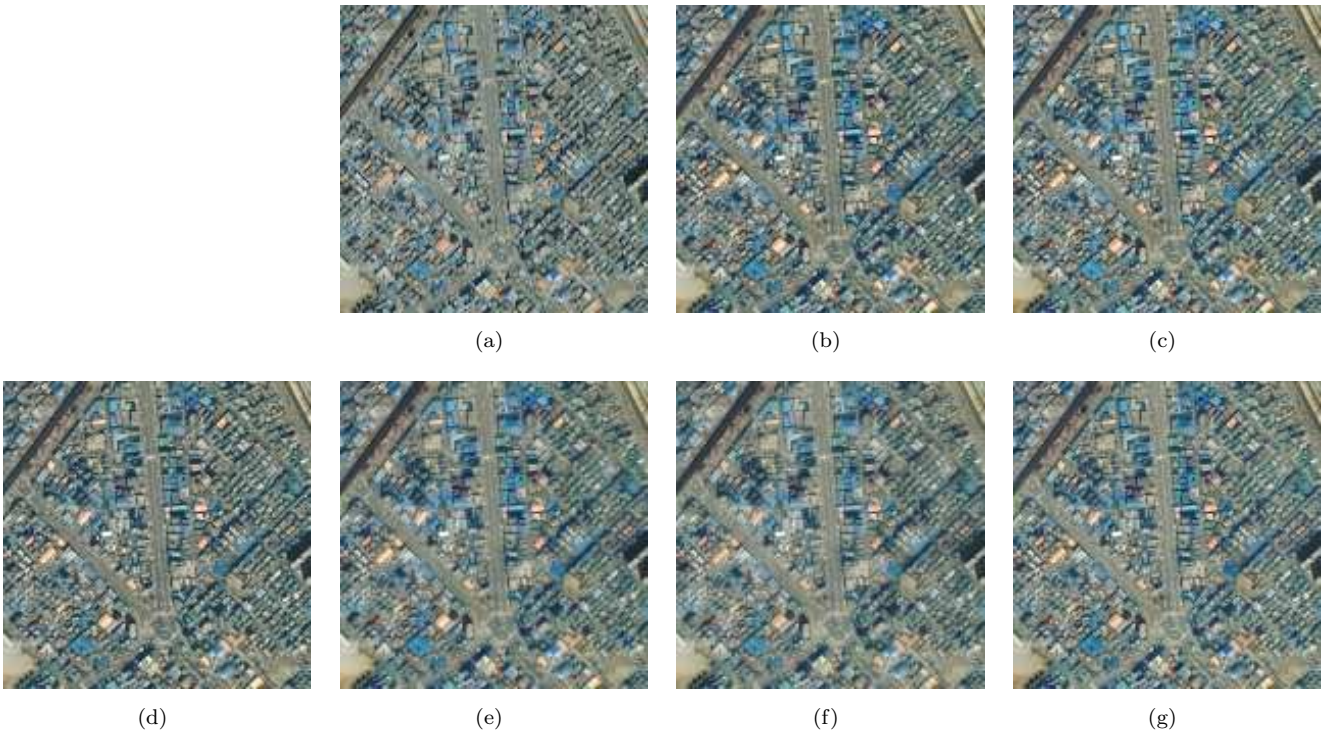

(a) (b) (c)

(d) (e) (f) (g)

Figure 4. Results for 2^{nd} IKONOS imagery: (a) original IKONOS color image(4m); (b) fused by the eFIHS; (c) fused by the eFIHS SA; (d) fused by the eFIHS SRF; (e) fused by the eFIHS TP; (f) fused by the eFIHS W; (g) fused by the proposed method.